


Article

# Image Denoising Based on Quantum Calculus of Local Fractional Entropy

Ala'a R. Al-Shamasneh<sup>1</sup> and Rabha W. Ibrahim<sup>2,3,\*</sup> 

<sup>1</sup> Department of Computer Science, College of Computer & Information Sciences, Prince Sultan University, Rafha Street, Riyadh 11586, Saudi Arabia

<sup>2</sup> Department of Computer Science and Mathematics, Lebanese American University, 1102 2801 Beirut, Lebanon

<sup>3</sup> Mathematics Research Center, Department of Mathematics, Near East University, Near East Boulevard, TRNC Mersin 10, Nicosia 99138, Turkey

\* Correspondence: rabhawaell.ibrahim@neu.edu.tr

**Abstract:** Images are frequently disrupted by noise of all kinds, making image restoration very challenging. There have been many different image denoising models proposed over the last few decades. Some models preserve the image's smooth region, while others preserve the texture margin. One of these methods is by using quantum calculus. Quantum calculus is a branch of mathematics that deals with the manipulation of functions and operators in a quantum mechanical setting. It has been used in image processing to improve the speed and accuracy of image-processing algorithms. In quantum computing, entropy can be defined as a measure of the disorder or randomness of a quantum state. The concept of local fractional entropy has been used to study a wide range of quantum systems. In this study, an image denoising model is proposed based on the quantum calculus of local fractional entropy (QC-LFE) to remove a Gaussian noise. The local fractional entropy is used to estimate the image pixel probability, while the quantum calculus is used to estimate the convolution window mask for image denoising. A processing fractional mask with  $n \times n$  elements was used in the suggested denoising algorithm. The proposed image denoising algorithm uses mask convolution to process each corrupted pixel one at a time. The proposed denoising algorithm's effectiveness is assessed using peak signal-to-noise ratio and visual perception (PSNR). The experimental findings show that, compared to other similar fractional operators, the proposed method can better preserve texture details when denoising.

**Keywords:** quantum calculus; local fractional entropy; fractional calculus; image denoising; fractional mask; symmetric window



**Citation:** Al-Shamasneh, A.R.; Ibrahim, R.W. Image Denoising Based on Quantum Calculus of Local Fractional Entropy. *Symmetry* **2023**, *15*, 396. <https://doi.org/10.3390/sym15020396>

Academic Editor: Juan Luis García Guirao

Received: 30 December 2022

Revised: 22 January 2023

Accepted: 28 January 2023

Published: 2 February 2023



**Copyright:** © 2023 by the authors. Licensee MDPI, Basel, Switzerland. This article is an open access article distributed under the terms and conditions of the Creative Commons Attribution (CC BY) license (<https://creativecommons.org/licenses/by/4.0/>).

## 1. Introduction

Symmetry in a mathematical functional equation refers to a transformation or operation, including the operators in fractional calculus, fractal and local fractional calculus that leave the equation unchanged. For example, if a functional equation is symmetric with respect to a particular group, it means that applying any element of that group to both sides of the equation results in another valid solution. In this way, symmetries can be used to generate new solutions to functional equations, and to understand the underlying structure of the problem.

Window masks are often used in image processing, as they have some useful properties that make them well suited for certain tasks. For example, they can be used to represent convolution kernels in image filtering. A window mask is a mathematical operation that modifies a signal by multiplying it with a window function. The window function is typically a locally defined function, such as a Gaussian or a rectangular function, which is centered on a particular point in the signal.

A local fractional operator is a mathematical operation that modifies a signal by applying fractional derivatives or integrals to it. Fractional calculus is a generalization of

standard calculus, which allows for noninteger powers of the differentiation or integration operator. The local fractional operator applies these fractional operations on a small localized region of the signal, rather than globally. It is possible that the term “window masks involving local fractional operator” refers to a specific technique in which the window mask is used, in combination with the local fractional operator to process a signal.

Digital images can be affected by various types of noise, which can degrade the quality of the image and make it difficult to interpret. Image noise, which is typically a component of electronic noise, is the random variation in image brightness. This means that the probability of the noise taking on a positive value is the same as the probability of it taking on a negative value. Examples of image noise include Gaussian noise and salt and pepper noise. Gaussian noise is a type of noise that is distributed according to a normal, or Gaussian distribution, which is a bell-shaped curve. Gaussian noise is commonly found in digital images, and can be caused by a variety of factors, such as electronic noise in the image sensor or transmission errors during image transmission. Salt and pepper noise is a type of noise that consists of isolated pixels that are either very bright or very dark. This type of noise is typically caused by extreme values in the image data, such as a very bright light source or a very dark shadow. Salt and pepper noise can be particularly noticeable in images that have a high dynamic range, as it can cause individual pixels to stand out from the rest of the image. Noise can be difficult to remove from an image, as it is evenly distributed throughout and cannot be easily isolated. However, various techniques such as image filtering and restoration can be used to reduce the impact of image noise on the image quality [1].

Preserving and enhancing the key features is one of the challenges faced during the denoising process. Edge is one of the most common and important features for images. Since both noises and edges contain high frequencies, linear filters typically do not provide satisfactory performance when denoising. Because of this, a few nonlinear filters have been suggested [2]. One traditional example is the median filter. Image filters based on wavelets are continuously evolving. Based on the relationship between the original image and the noise, there are two types of noise: additive noise and multiplicative noise. Adding the noise field to the original image is known as additive noise. The category of additive noise is most frequently found in the actual scene. In contrast, in multiplicative noise models, the original image is multiplied by the noise field.

Noise reduction has traditionally relied on linear models. In flat areas of images, these methods work well; their limitation, however, is that they cannot keep the edges well. However, the nonlinear model can handle edges more effectively than linear models. Many researchers have recently used fractional calculus theory to process images [3–5]. Numerous fields of the engineering sciences depend on fractional calculus and its applications [3,4,6,7]. In this study, a new denoising model based on the quantum calculus of local fractional entropy (QC-LFE) is proposed to obtain high fidelity of the denoised images with additive white Gaussian noise (AWGN). In quantum calculus, the concept of entropy is used to describe the amount of uncertainty or disorder in a system, and local entropy is used to measure this uncertainty in specific regions of the system. A straightforward and a window mask is suggested for the restoration of noisy images, in order to solve the model effectively and consistently. In actuality, image denoising is a well-known issue that has been researched for a very long time, and is still a difficult and unfinished task.

To apply the proposed model for removal of multiplicative noise, local fractional entropy is used to estimate the image pixel probability, while the quantum calculus is used to estimate the convolution window mask for image denoising [8]. According to experimental findings, the suggested method restores images effectively, especially when it comes to edge enhancement and preservation. In fact, the amount of information in an image is measured by its image entropy. There is more information in the image the lower the entropy. The entropy of original image and image with noise is illustrated in Figure 1. This illustration confirms that the entropy of original image has less value than the entropy of image with noise. This motivates us to investigate an efficient image denoising

algorithms to overcome the limitations of the existing denoising methods by applying the new QC-LFE. The neighborhood information feature of the image in the spatial domain is used by the denoising method to remove the noise by the quantum local fractional entropy window mask. The finding of this study serves as a guide for future work on image denoising using fractional quantum calculus.

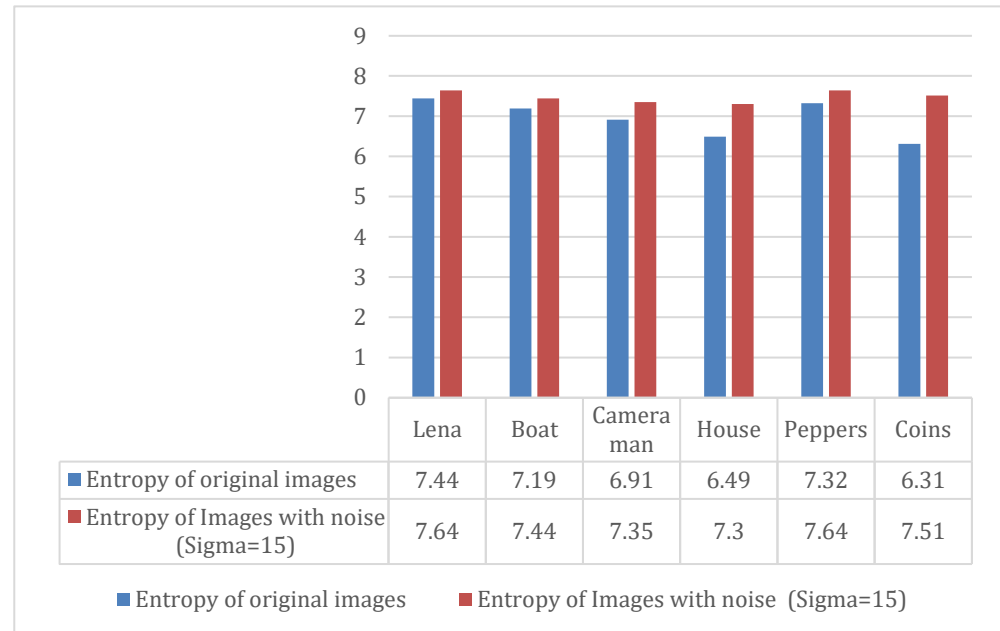


**Figure 1.** The entropy values of original images and images with noise.

## 2. Related Works

Image denoising is the process of restoring a digital image that has been corrupted by noise of any kind. Image denoising method based on fractional calculus has been widely researched. The study of using the convex solution of heat equation in fractional calculus for image denoising has been proposed by [9]. This study reviews various types of special equations, such as fractal heat transfer, heat conduction equation and the fractional sub-diffusion equation. The major problem identified is how to manage the image denoising using the fractional heat diffusion concept. This study gives a solution for denoising different Gaussian noise values on grayscale and color images. This algorithm achieved a PSNR of 29.87 on a grayscale ‘Cameraman’ image.

The fractional polynomials of the Alexander method for image denoising were accordingly proposed by [10]. On eight directions, structures for  $n \times n$  fractional mask windows were created for image denoising. This study reviews various methods using fractional polynomials to find an improved solution for removing noise in images. The major problem identified is how to manage the over smooth noisy images. This study gives a solution for denoising the Gaussian noise in grayscale and color images. The final denoising performances achieved higher visual interpretation measured by using the PSNR values.

Moreover, the approximate fractional Cauchy-Euler equation-based image denoising method was proposed by [7]. Based on this approach, a new fractional mask was introduced to enforce the image denoising based on the solution of the fractional Cauchy-Euler equation. This study reviews several complex-step approximation methods applied in signal and image processing. The major problem identified in this study is how to achieve a higher PSNR by making use of a fractional mask depending on the approximate analytic solution of Cauchy-Euler equations. The final denoising performances achieved higher visual interpretation measured by using the PSNR values. This algorithm achieved a PSNR of 29.32 on the grayscale ‘House’ image.

Likewise, Tsallis entropy was proposed by [11] as a new image denoising model focusing on image detail restoration using  $n \times n$  fractional mask. This study analyses some denoising methods using the fractional derivatives. The major problem acknowledged in how to apply two fractional Riesz filter mask windows in the x and y directions to achieve higher noise decreasing. The convolution of Tsallis entropy with the Riesz fractional derivative for image denoising on different Gaussian noise values is solved in this study. This algorithm achieved a PSNR of 9.98 on the grayscale 'Boat' image.

In addition, sophisticated strategies such as adaptive fractional order anisotropic diffusion have been used in image denoising by [12]. The local variance reflects the complexity of the local image texture in this approach, and the fractional differentiation order is selected in an adaptive manner. This study reviews several approaches applied based on fractional order partial differential. The major problem identified in this study is how to improve the image denoising, keeping texture information, good visual effects and detailed image information. This algorithm achieved a PSNR of 9.98 on grayscale 32.33 on the 'Lena' image. Some remarkable attentions, namely the conformable fractional calculus (CFC), was applied for image denoising by [13]. The CFC window structures are suggested by four masks for the x and y directions.

This study reviews several approaches applied on multiplicative image noise based on conformable fractional calculus. The major problem identified in this study is how to improve the image denoising by applying the CFC filter. This algorithm offered satisfactory PSNR results. The measured PSNR was achieved better results compared with other denoising algorithms. Very recently, a study by [14] proposed an adaptive fractional integral operator using different type of entropies to improve the fractional masks. This study reviews several approaches on Atangana–Baleanu fractional order derivatives. The major problem identified in this study is how to preserve as much of the image's edge and texture details as possible. This algorithm was achieved satisfactory PSNR results on using the adaptive order function. The experimental results showed that the proposed fractional denoising achieved a PSNR of 30.94 on the 'Cameraman' image. However, applying fractional calculus techniques took advantage of the similarities in the denoising outcomes.

Recently, deep learning techniques have been created to address this issue [15]. Cheng Yao et al. [16] proposed blind denoising methods based on deep learning using a multi-scale residual fusion network. This study reviews various image denoising methods that used deep learning approaches. The major problem identified in this study is how to preserve the edge and texture details of the image as much as possible by applying the multi-scale residual fusion network. The experimental results showed that the proposed deep-learning method achieved a PSNR of 30.82 on the 'House' image.

The goal of image denoising is to eliminate noise, and thereby restore the original image. However, it can be challenging to distinguish the noise, edge and texture during the denoising process, so that the denoised images may inevitably lose some details. In general, the research gaps are how to recover important information from noisy images during the noise removal process, in order to produce high-quality images.

Considering the above review, most existing denoising methods do not perform well for restoring the true image. Furthermore, obtaining high-quality images requires the removal of noise, which is a significant problem today; it is hence inspired by the special properties of QC-LFE for image denoising, which can preserve edge and texture in images. This is promising, as QC-LFE determines the pixel probability by the local fractional entropy in quantum calculus, which can solve the nonlinear image denoising problem. The major contributions of the study are:

- (1) A necessary summary of the theory behind fractional quantum calculus has been derived.
- (2) A new algorithm based on new QC-LFE is proposed to remove the additive white Gaussian noise (AWGN).
- (3) Numerous experiments are carried out to show that the proposed method outperforms cutting-edge techniques in the additive white Gaussian noise (AWGN) denoising.

### 3. Methods

This section is devoted into the following subsections. Rendering to the recommended model, local fractional entropy is utilized by the input’s pixel regularity. The model that was then exhibited enhanced every pixel, with the modifications in the gray levels consuming no impression on the high occurrence specifics.

#### 3.1. Local Fractional Calculus

The local fractional integral has a modest description assumed a dependable function  $h(w) \in [a, b]$  [17–19]

$$H^{(\mu)}h(w) = \frac{1}{\Gamma(1 + \mu)} \int_a^b h(w)(dw)^\mu, \tag{1}$$

where  $\Gamma$  is the Euler gamma function and  $\mu \in (0,1)$  is the fractional power operator.

The discrete custom of (1) is expressed by

$$H^{(\mu)}h(w) = \frac{1}{\Gamma(1 + \mu)} \lim_{\Delta w_m \rightarrow 0} \sum_{m=0}^{n-1} h(w_m) (\Delta w_m)^\mu, \tag{2}$$

where:

$$\Delta w_m = w_{m+1} - w_m, \quad w_0 = a \leq \dots \leq b = w_n .$$

#### 3.2. Local Fractional Entropy

Researchers have recently promoted utilizing fractional entropies to deal with fractional nonlinear problems [17,20,21]. Tsallis entropy, or local fractional entropy, is used to improve the fractional integral operator, which is described as follows

$$E_\nu(h(w)) = \frac{\int_a^b (h(w))^\nu dw - 1}{1 - \nu} \tag{3}$$

where  $h$  in  $(0,1)$  indicates the probability of the pixel ( $w$ ). Hence, in the discrete form this can be seen as follows:

$$E_\nu(h(w)) = \frac{1}{1 - \nu} \left( \sum_{m=0}^{n-1} (h(w_m))^\nu - 1 \right), \quad \nu \neq 1. \tag{4}$$

The following is created by using the derivative about  $h(w_m)$  in Equation (4):

$$(E_\nu(h(w)))' = \frac{\nu}{1 - \nu} \sum_{m=0}^{n-1} h^{\nu-1}(w_m) \tag{5}$$

The power function in Equation (5) causes the following local fractional integral:

$$H^{(\mu)}h^\nu(w) = \lim_{\Delta w_m \rightarrow 0} \sum_{m=0}^{n-1} \frac{h^\nu(w_m)(\Delta w_m)^\mu}{\Gamma(1 + \mu)}. \tag{6}$$

By using the fact  $\Delta w_m = 1$ , we have:

$$H^{(\mu)}h^\nu(w) = \sum_{m=0}^{n-1} \frac{h^\nu(w_m)}{\Gamma(1 + \mu)}. \tag{7}$$

By taking the derivative about  $h(w)$  for the two sides of Equation (7), the following is realized:

$$\left( H^{(\mu)}h^\nu(w) \right)' = \nu \sum_{m=0}^{n-1} \frac{h^{\nu-1}(w_m)}{\Gamma(1 + \mu)} \tag{8}$$

By assuming  $\mu = \nu \in [0,1)$ , the local fractional entropy for images is the convolution of Equations (5) and (8):

$$U_\mu = ( H^{(\mu)} h^\mu(w) )' * ( E_\mu(h(w_m)) )' \tag{9}$$

Accordingly, the local fractional operator is developed. Consequently, we obtain the following summation:

$$U_\mu = \frac{\mu^2}{(1-\mu)} \left( \sum_{m=0}^{n-1} \frac{h^{\mu-1}(w_m)}{\Gamma(1+\mu)} \right), \quad h(w_m) \neq 0 \tag{10}$$

The term  $h(w_m)$  symbolizes the image probability of the pixel  $w_m$ . From Equation (10), the m-coefficient is as follows

$$(U_\mu)_m = \frac{\mu^2}{(1-\mu)\Gamma(1+\mu)} h_m^{\mu-1}, \quad m = 0, 1, 2, \dots, \tag{11}$$

where  $h_m = h(w_m)$ . Note that  $(U_\mu)_m \in [0,1]$ , where  $\mu \in [0,0.6]$ .

We have the following fractal entropy coefficients:

$$(U_\mu)_0 = \frac{\mu^2}{(1-\mu)\Gamma(1+\mu)} h_0^{\mu-1}, \tag{12}$$

$$(U_\mu)_1 = \frac{\mu^2}{(1-\mu)\Gamma(1+\mu)} h_1^{\mu-1},$$

$$(U_\mu)_2 = \frac{\mu^2}{(1-\mu)\Gamma(1+\mu)} h_2^{\mu-1}$$

### 3.3. The Quantum Calculus (q-Calculus)

In the q-calculus, where  $q \in (0,1)$ , the quantum number is presented as follows [22–26]:

$$[v]_q = \frac{q^v - 1}{q - 1}.$$

Since  $\Gamma(1+v) = v!$ , then by consuming the q-number, we have  $\Gamma_q(1+v) = [v]_q!$ , where  $[v]_q!$  is the q-factorial defined as follows:

$$[v]_q! = \frac{(1-q)^v}{(1-q^v)(1-q^{v-1}) \dots (1-q)}$$

Using  $\Gamma_q(1+v) = [v]_q!$  in (11) to obtain the m-coefficient of q-local fractional entropy (q-LFE)

$$\begin{aligned} (U_{q,\mu})_m &= \frac{\mu^2}{(1-\mu)\Gamma_q(1+\mu)} h_m^{\mu-1}, \quad m = 0, 1, 2, \dots, n-1, \quad q \in (0,1) \\ &= \left( \frac{\mu^2}{(1-\mu)[\mu]_q!} \right) h_m^{\mu-1} \\ &= \left( \frac{\mu^2(1-q^\mu)(1-q)}{(1-\mu)(1-q)^\mu} \right) h_m^{\mu-1}, \quad \mu \in (0,1), \end{aligned}$$

such that the first three coefficients are:

$$(U_{q,\mu})_0 = \left( \frac{\mu^2(1-q^\mu)(1-q)}{(1-\mu)(1-q)^\mu} \right) h_0^{\mu-1},$$

$$(U_{q,\mu})_1 = \left( \frac{\mu^2(1-q^\mu)(1-q)}{(1-\mu)(1-q)^\mu} \right) h_1^{\mu-1},$$

$$(U_{q,\mu})_2 = \left( \frac{\mu^2(1-q^\mu)(1-q)}{(1-\mu)(1-q)^\mu} \right) h_2^{\mu-1}$$

One potential application of quantum calculus in image processing is in the development of algorithms for image compression. By representing images as quantum states, it may be possible to develop more efficient algorithms for image compression that take advantage of the principles of quantum mechanics [27–30]. Another potential application of quantum calculus in image processing is in the development of algorithms for image recognition and classification. By representing images as quantum states, it may be possible to develop algorithms that can more accurately and efficiently identify and classify objects in images. It is important to note that quantum calculus is an active area of research, and many of the potential applications of quantum calculus in image processing are still being explored and developed [31–34]. In this investigation, we add more applications of the quantum calculus in image processing by enhancing the images.

### 3.4. The Proposed Method

The proposed image denoised algorithm is given by

$$T_q = I_{noisy} * W_{3 \times 3}(U_{q,\mu})_m, \quad m = 0, 1, 2 \tag{13}$$

where \* indicates the convolution product and  $W_{3 \times 3}$  is the window mask of dimension  $3 \times 3$  with the quantum coefficients. In this study, the proposed mask is organized as follows:

$$W_{q,\mu} = \begin{bmatrix} (U_{q,\mu})_2 & (U_{q,\mu})_0 & (U_{q,\mu})_2 \\ (U_{q,\mu})_0 & (U_{q,\mu})_1 & (U_{q,\mu})_0 \\ (U_{q,\mu})_2 & (U_{q,\mu})_0 & (U_{q,\mu})_2 \end{bmatrix}$$

$$= \begin{bmatrix} \frac{\mu^2(1-q^\mu)(1-q)}{(1-\mu)(1-q)^\mu} h_2^{\mu-1} & \frac{\mu^2(1-q^\mu)(1-q)}{(1-\mu)(1-q)^\mu} h_0^{\mu-1} & \frac{\mu^2(1-q^\mu)(1-q)}{(1-\mu)(1-q)^\mu} h_2^{\mu-1} \\ \frac{\mu^2(1-q^\mu)(1-q)}{(1-\mu)(1-q)^\mu} h_0^{\mu-1} & \frac{\mu^2(1-q^\mu)(1-q)}{(1-\mu)(1-q)^\mu} h_1^{\mu-1} & \frac{\mu^2(1-q^\mu)(1-q)}{(1-\mu)(1-q)^\mu} h_0^{\mu-1} \\ \frac{\mu^2(1-q^\mu)(1-q)}{(1-\mu)(1-q)^\mu} h_2^{\mu-1} & \frac{\mu^2(1-q^\mu)(1-q)}{(1-\mu)(1-q)^\mu} h_0^{\mu-1} & \frac{\mu^2(1-q^\mu)(1-q)}{(1-\mu)(1-q)^\mu} h_2^{\mu-1} \end{bmatrix} \tag{14}$$

Note that  $h_m$  indicates the probability of the pixel. The pixel probability was calculated by utilizing the pixels’ histogram technique, which converts the distribution of pixel intensities into a discrete distribution of probabilities. The pixel probability is given by dividing each histogram value (pixelCounts) by the total number of pixels. Since a digital image is a discrete set of values, it can be thought of as a matrix, so that the pixel probability is equivalent to dividing pixelCounts by the image size in pixels as given: prob = pixelCounts/(rows\*colm).

The mask window’s size should be minimal, in order to achieve high denoising PSNR. The following are the steps for the proposed fractional QC-LFE mask window image denoising algorithm as shown in Figure 2.

1. The fractional QC-LFE mask window mask windows with  $3 \times 3$  sizes are initialized using (14).
2. The values  $u$  and  $q$  of the fractional parameter operator are empirically fixed  $\mu, q \in (0,1)$ .
3. To evaluate how well the proposed algorithm works, white Gaussian noise with  $\sigma$  of 15, 20, 25 and 30 is added.
4. The corrupted image’s pixels are convolved with the mask windows using (13).
5. The noise was then removed from the corrupted images using the proposed and Gaussian filters.
6. The PSNR was used to measure the denoising process’ effectiveness.
7. The same algorithm can be used for color images, but each of the red, green and blue color components is implemented separately.

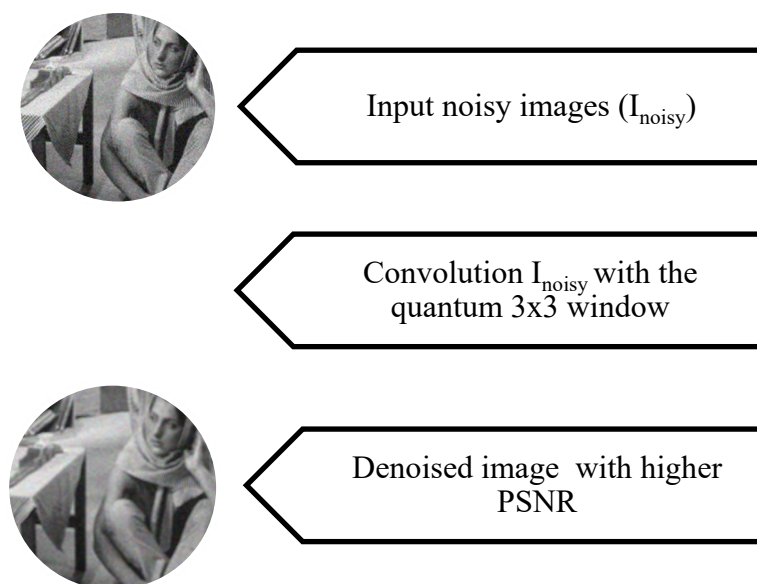


Figure 2. Proposed algorithm.

#### 4. Experimental Results

The results of proposed denoising method are achieved by using MATLAB R2021b. In the experiments, the collections of images involved grayscale images (Lena, Boat, Cameraman, Peppers and Coins) and color images (House, Peppers, Zebra and Barbara). The default Gaussian noise is added into the image with different noise sigma noise levels ( $\sigma = 15, 20, 25, 30$ ). The window mask of the suggested method is given in a  $3 \times 3$  pixels window.

In this study, the PSNR is used as a trade span for the ratio between the input image and the denoised image. The PSNR is most typically used to measure the image quality of image denoising. The higher the PSNR score, the more efficient the denoising algorithm. The PSNR is given by

$$PSNR = 10 \cdot \log_{10} \left( \frac{M^2}{MSE} \right) \quad (15)$$

where M is the maximum value of the pixel and MSE is the mean square error between the original (I) and denoised image (T), and is given by:

$$MSE = \frac{1}{m \cdot n} \sum_{i=0}^{m-1} \sum_{j=0}^{n-1} [I(i, j) - T(i, j)]^2 \quad (16)$$

The denoising approach consists of two main steps to analyze the proposed QC-LFE window mask-based denoising model:

- Apply a standard Gaussian filter to denoise the color and grayscale testing images.
- Use the proposed QC-LFE-based model to denoise the color and grayscale testing images.
- The following steps are involved in the processes of the above two mentioned stages:
- Add Gaussian noise with variances of 15, 20, 25 and 30.
- Determine the PSNR for color and grayscale test images with various noise variances.
- Determine the entropy for color and grayscale test images with various noise variances.

The denoising qualitative performance of the testing images under the noise level of  $\sigma = 15$  is illustrated in Figure 3, Figure 4 shows the PSNR of the results of a test of denoising using grayscale images with Gaussian noise levels of 15. Figure 5 shows, for grayscale images, the entropy of the testing denoising result. Figure 6 shows the PSNR of the results of a test of denoising using color images with Gaussian noise levels of 15. Figure 7 shows the entropy of the results of testing the denoising of color images using Gaussian noise levels of 15.



Figure 8 shows the results of the testing with 20 Gaussian noise levels. Figure 9 shows the PSNR of the results of a test to denoise grayscale images using Gaussian noise levels. Figure 10 shows the entropy of the test denoising result using grayscale images with Gaussian noise levels of 20. Figure 11 shows the PSNR of the denoising test results using color images with a Gaussian noise level of 20. Figure 12 shows the entropy of the denoising test results for color images using a Gaussian noise level of 20.

Figure 13 shows the results of the testing with 25 Gaussian noise levels. Figure 14 shows the PSNR of the test denoising result using grayscale images and a Gaussian noise level of 25. Figure 15 shows the entropy of the test denoising result for grayscale images using Gaussian noise levels of 25. Figure 16 shows the PSNR of the denoising test results using color images with a Gaussian noise level of 25. Figure 17 shows the entropy of the denoising test result for color images using a Gaussian noise level of 25.

Figure 18 shows the results of the testing with 30 Gaussian noise levels. Figure 19 shows the PSNR of the test denoising result using grayscale images with Gaussian noise levels of 30. Entropy of the test denoising result using Gaussian noise levels of 30 for grayscale images is shown in Figure 20. The PSNR of the testing denoising outcome using Gaussian noise levels of 30 for color images is shown in Figure 21. The entropy of the test denoising outcome using Gaussian noise levels of 30 for color images is shown in Figure 22.



Figure 3. Cont.

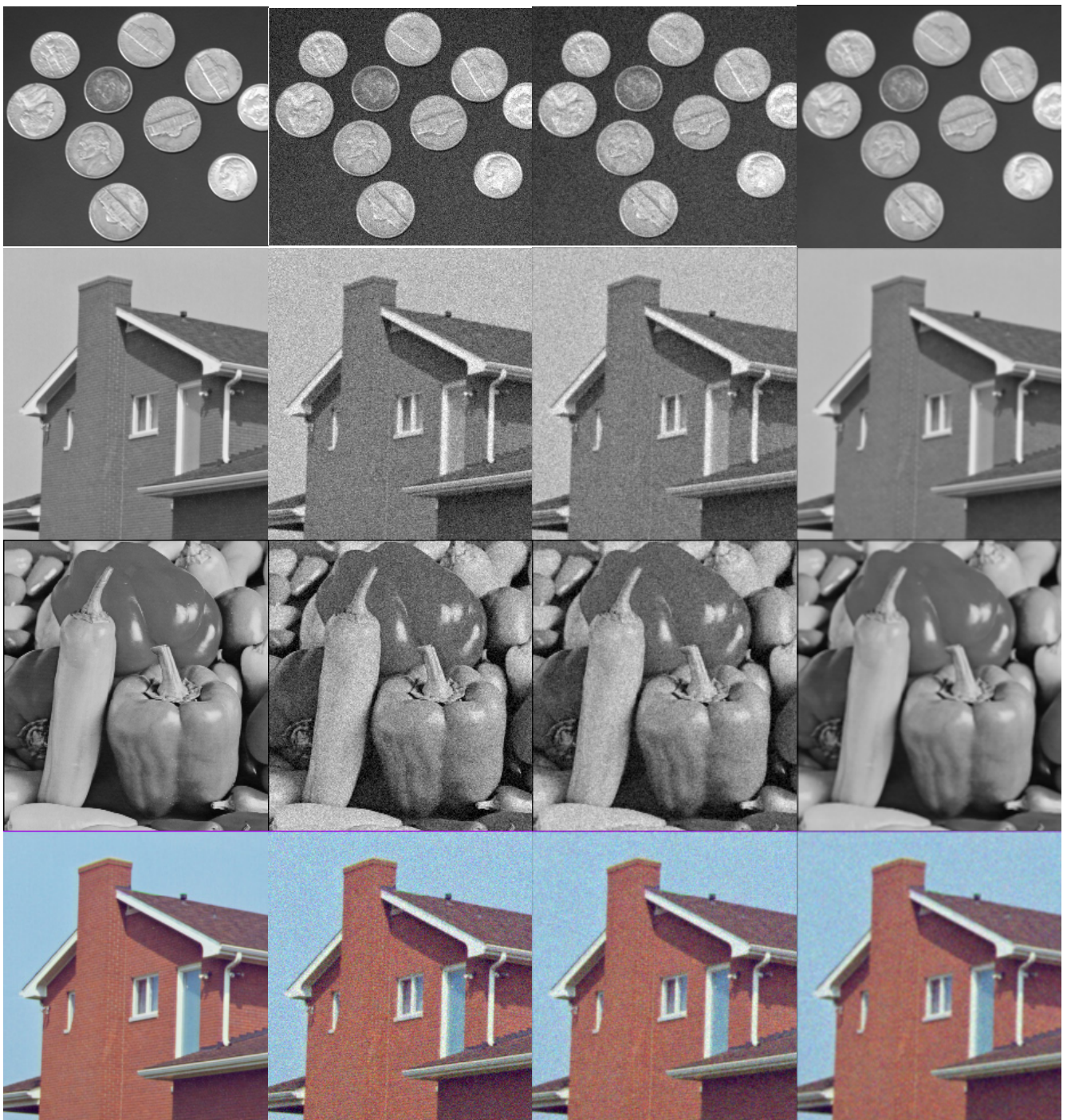


Figure 3. Cont.

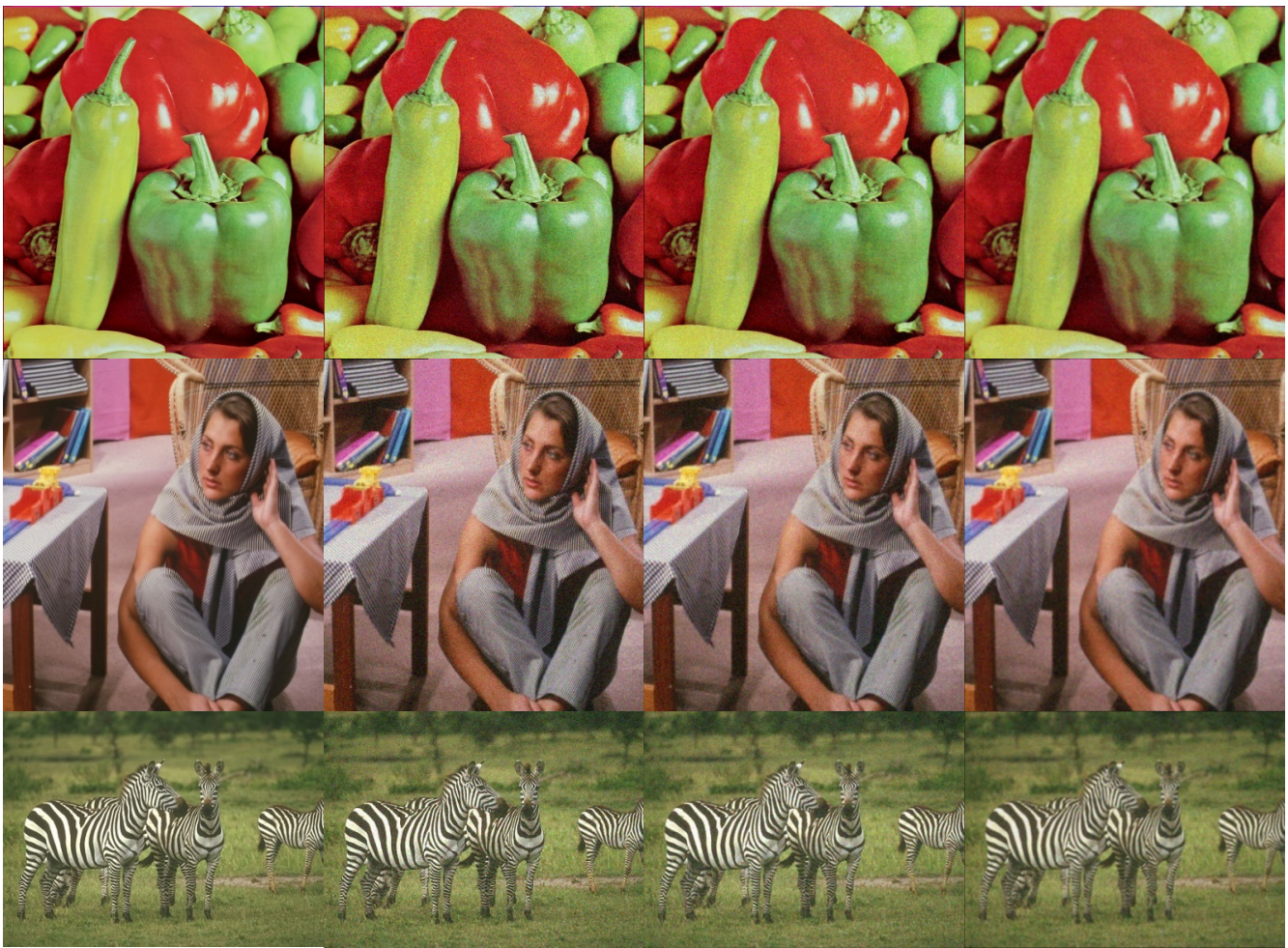


Figure 3. The testing denoising result using Gaussian noise levels ( $\sigma = 15$ ).

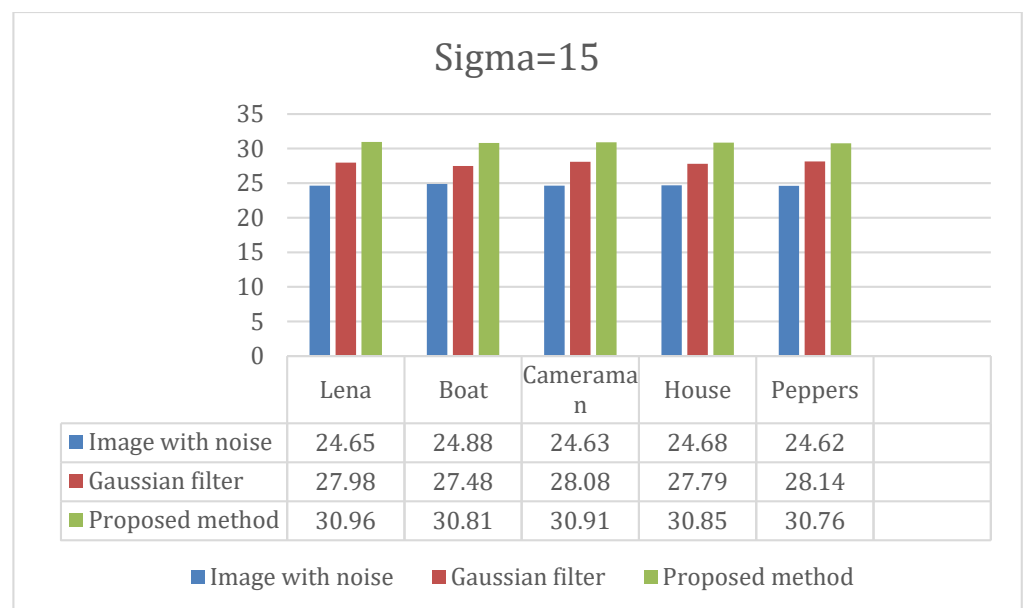
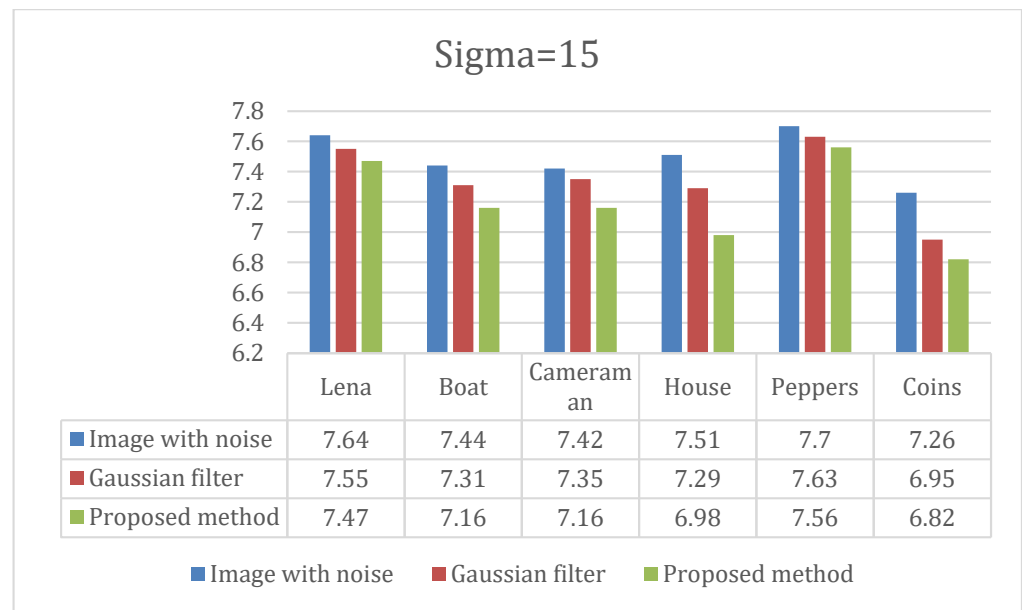
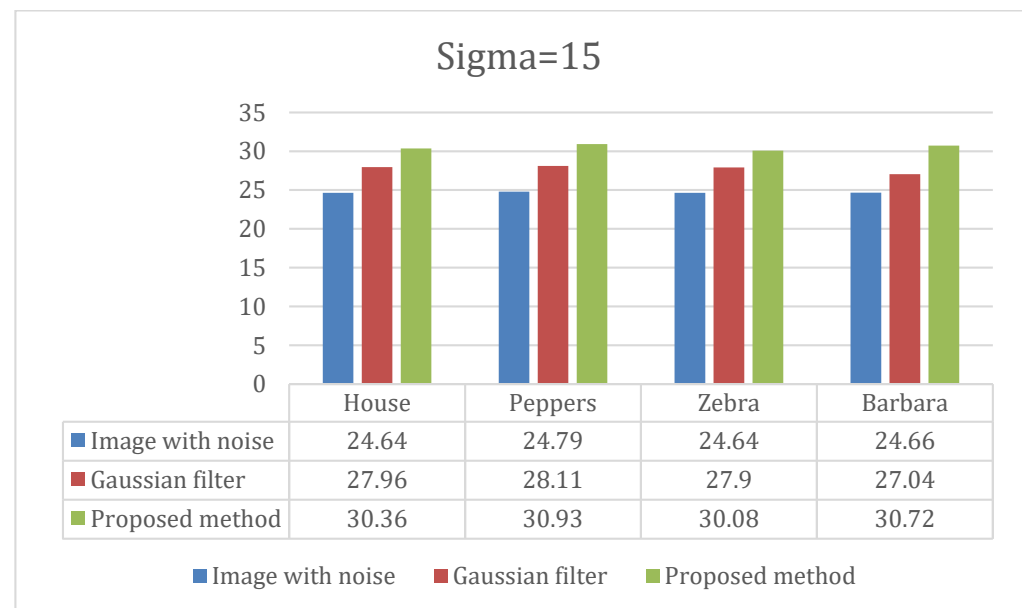


Figure 4. The PSNR of testing denoising result using Gaussian noise levels ( $\sigma = 15$ ) for grayscale images.



**Figure 5.** The entropy of testing denoising result using Gaussian noise levels ( $\sigma = 15$ ) for grayscale images.



**Figure 6.** The PSNR of testing denoising result using Gaussian noise levels ( $\sigma = 15$ ) for color images.

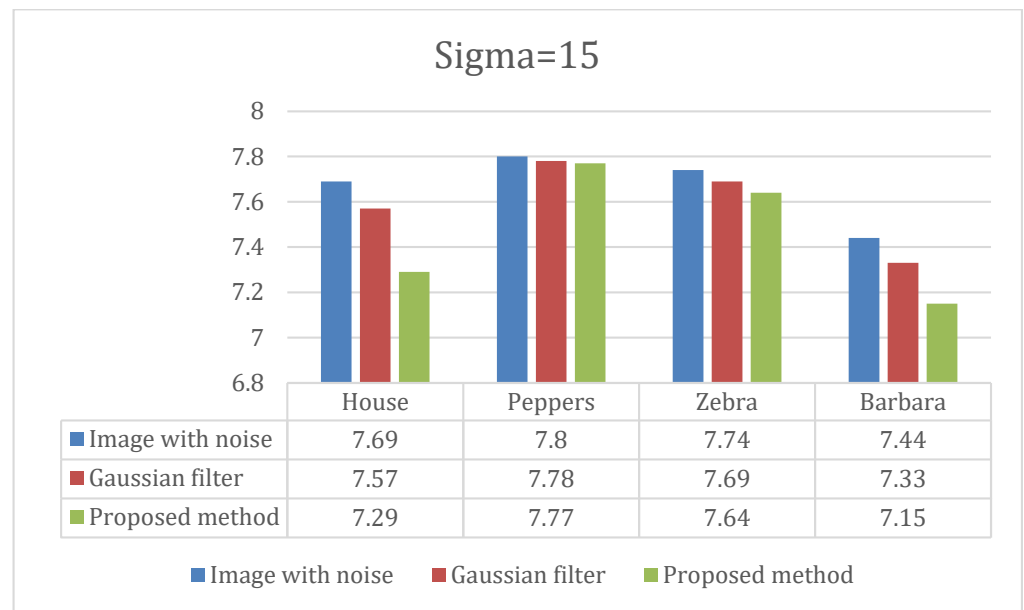


**Figure 7.** The entropy of testing denoising result using Gaussian noise levels ( $\sigma = 15$ ) for grayscale images.



**Figure 8.** Cont.

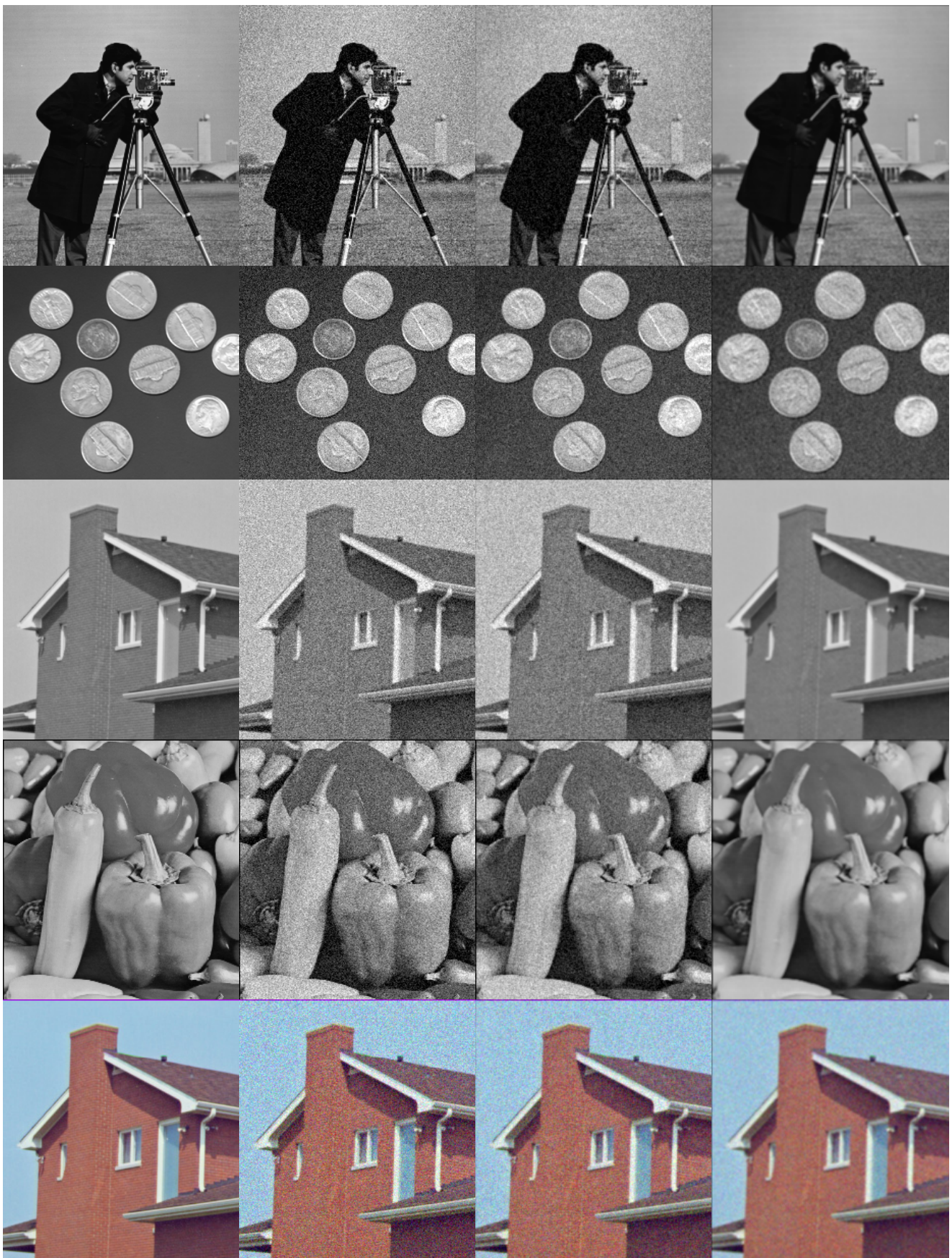


Figure 8. Cont.

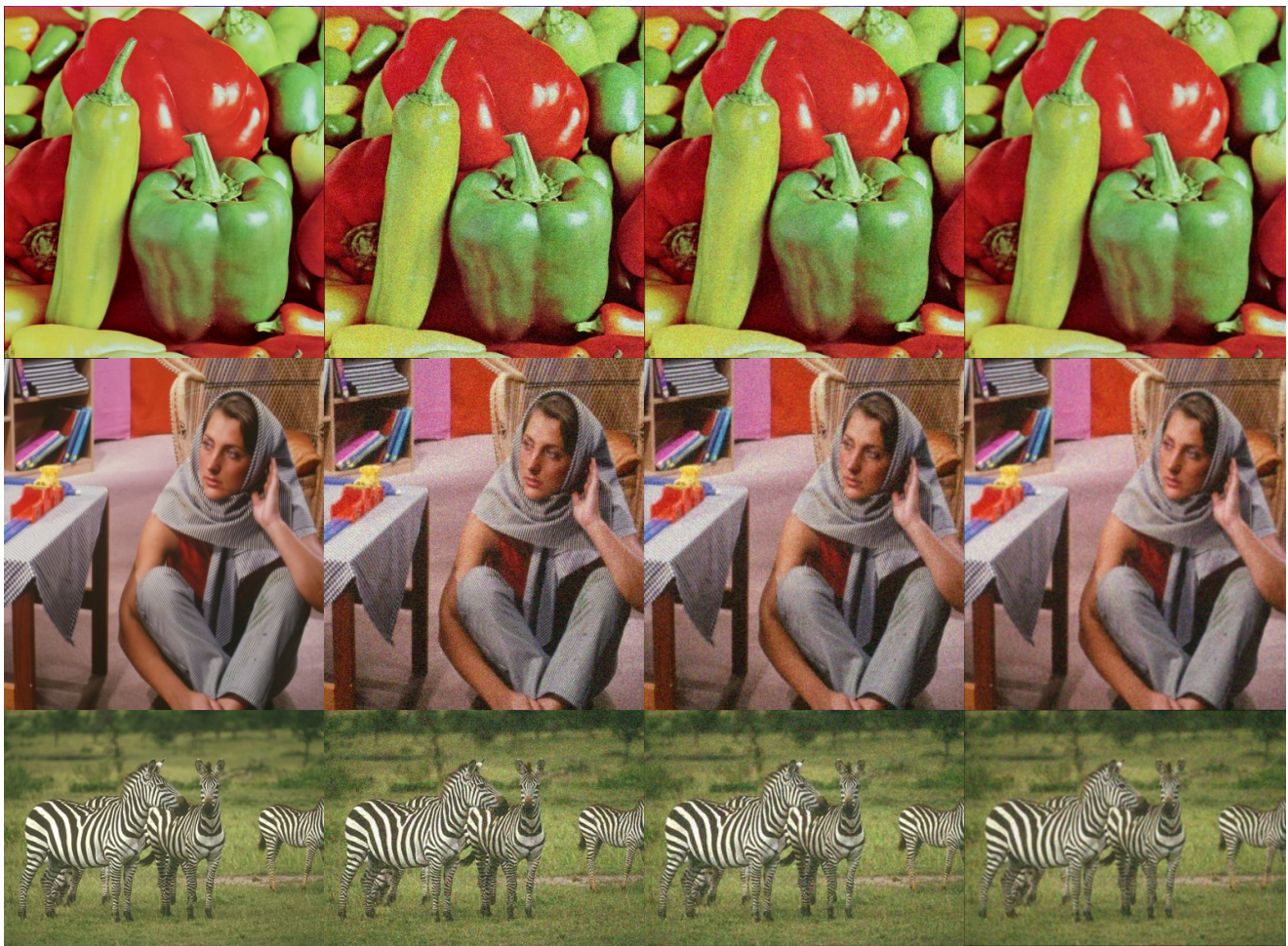


Figure 8. The testing denoising result using Gaussian noise levels ( $\sigma = 20$ ).

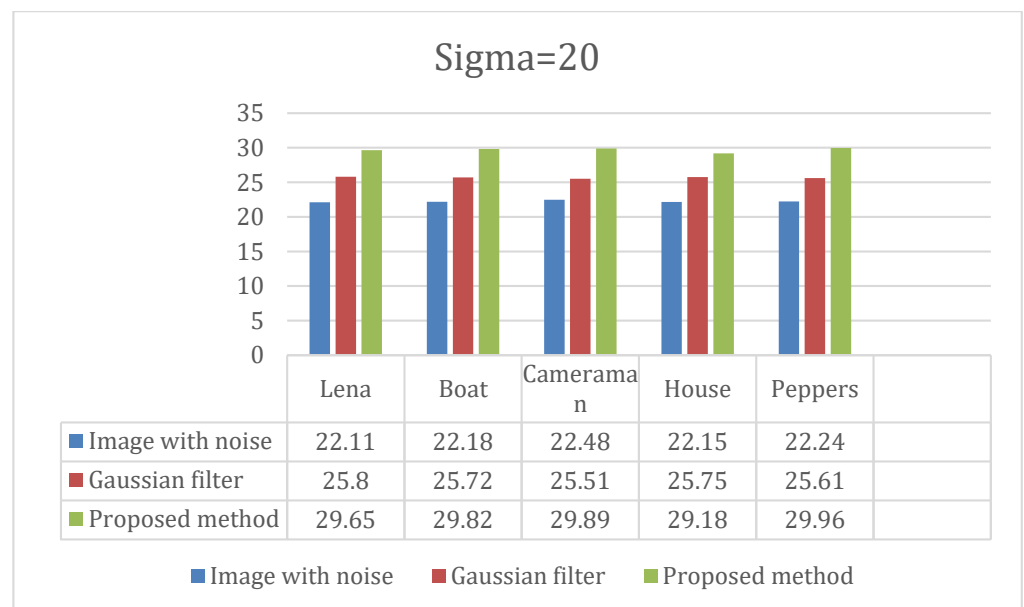
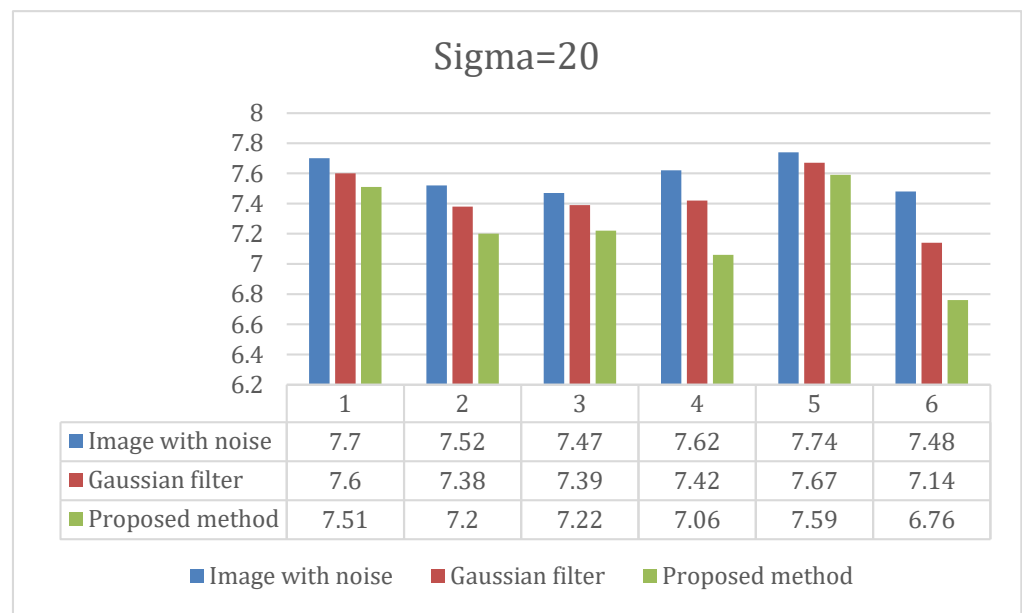
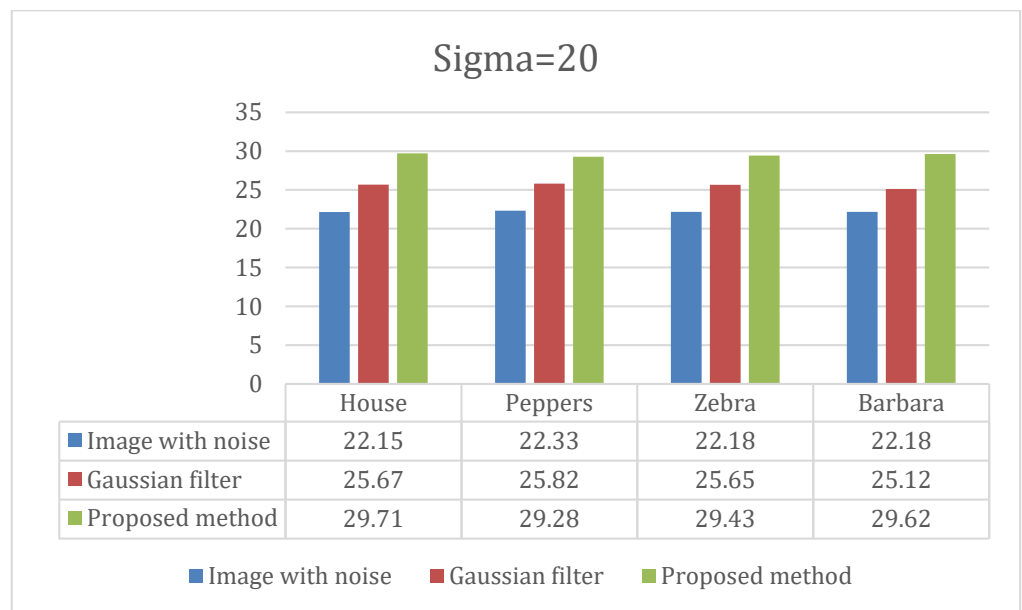


Figure 9. The PSNR of testing denoising result using Gaussian noise levels ( $\sigma = 20$ ) for grayscale images.



**Figure 10.** The entropy of testing denoising result using Gaussian noise levels ( $\sigma = 20$ ) for grayscale images.



**Figure 11.** The PSNR of testing denoising result using Gaussian noise levels ( $\sigma = 20$ ) for color images.



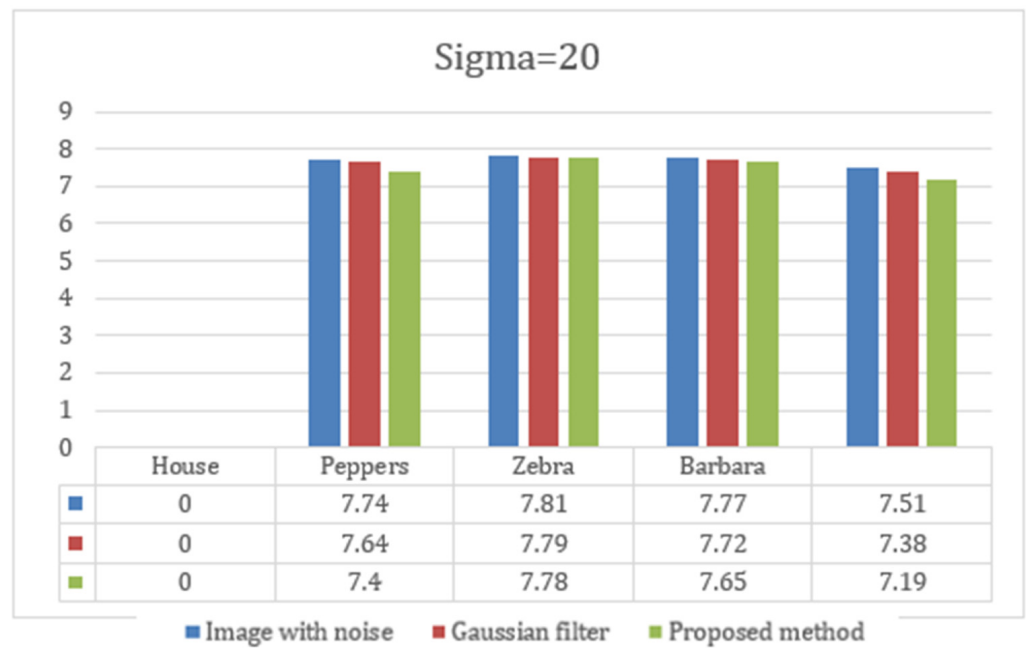


**Figure 12.** The entropy of testing denoising result using Gaussian noise levels ( $\sigma = 20$ ) for color images.



**Figure 13.** *Cont.*

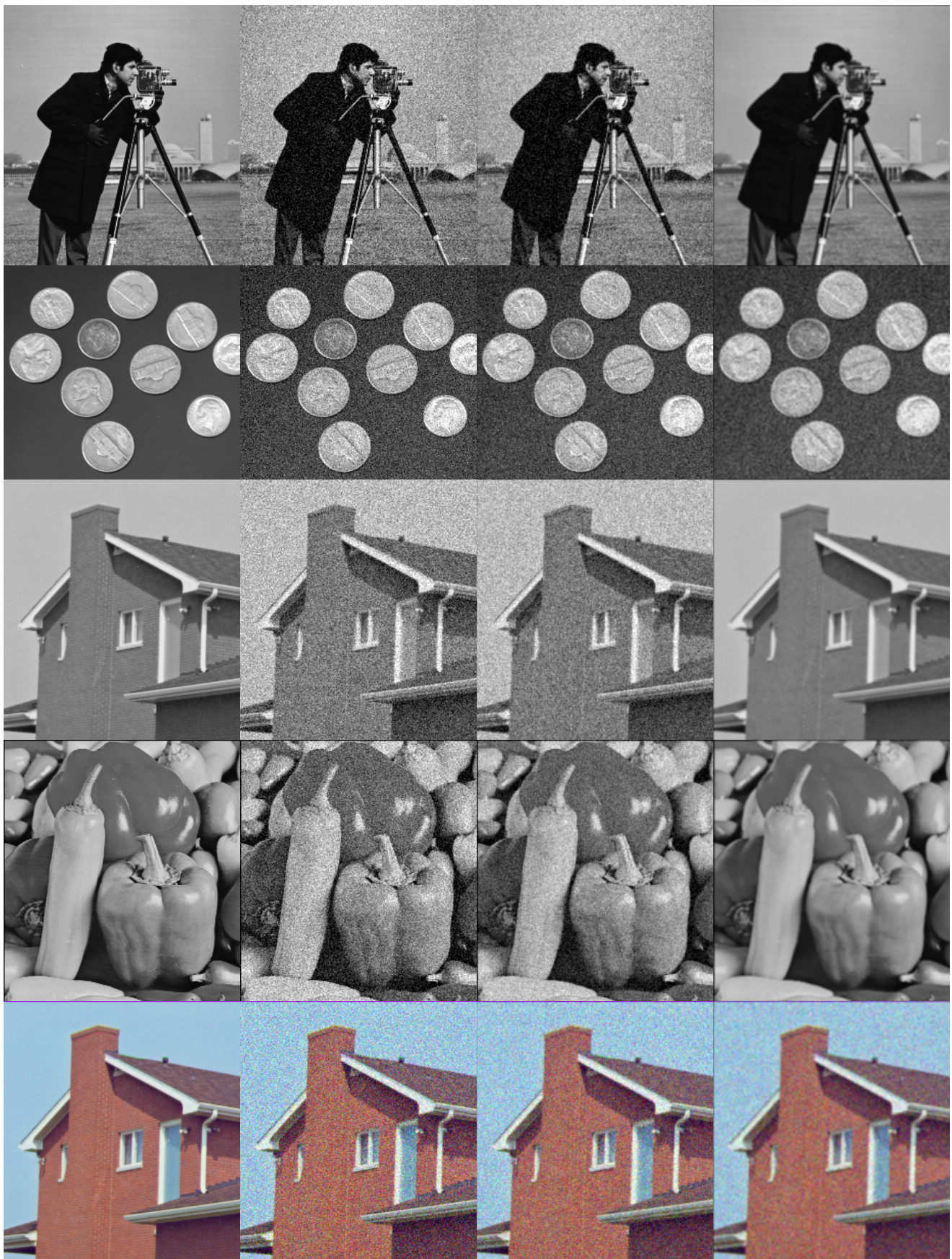


Figure 13. Cont.

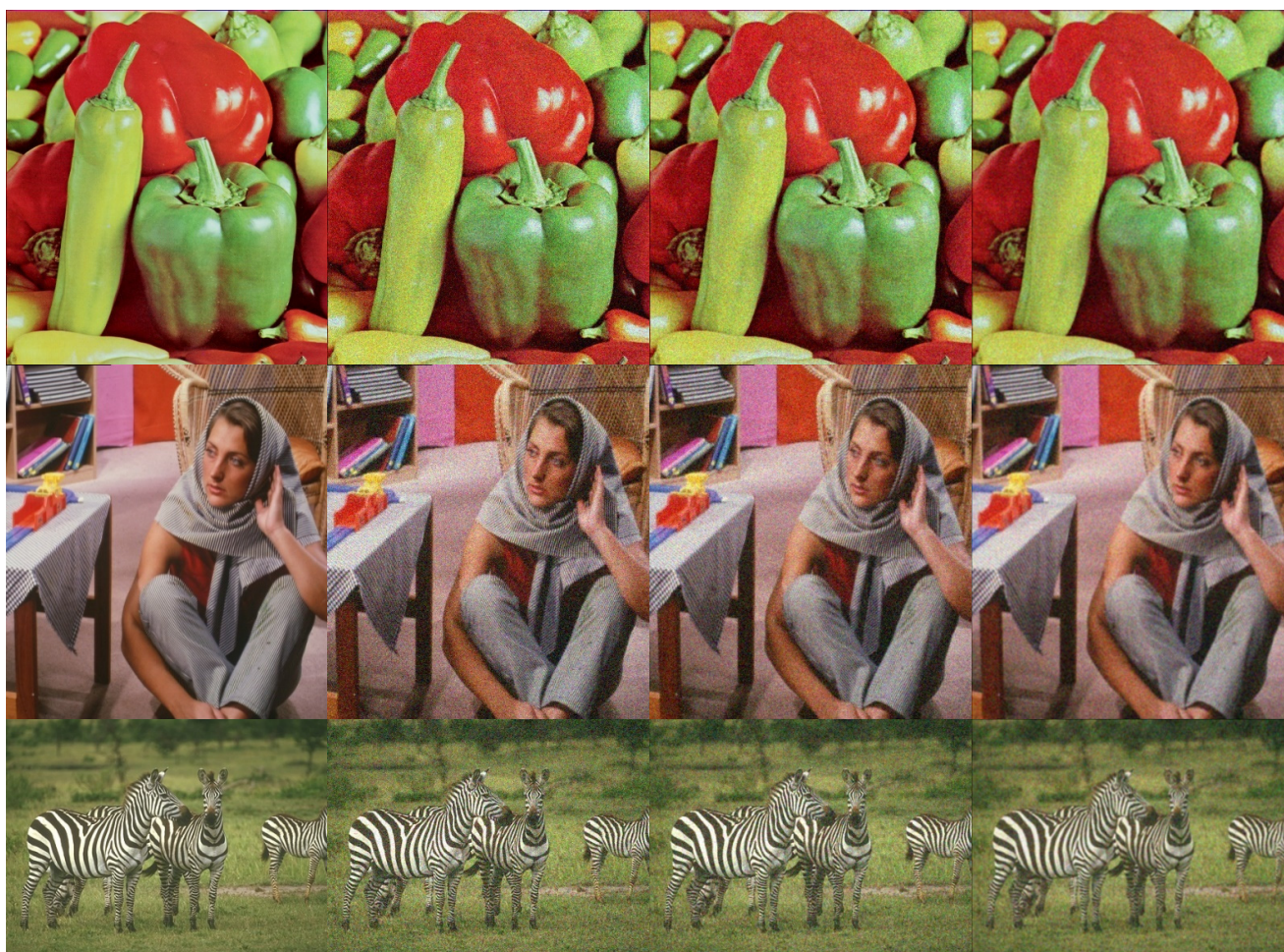


Figure 13. The testing denoising result using Gaussian noise levels ( $\sigma = 25$ ).

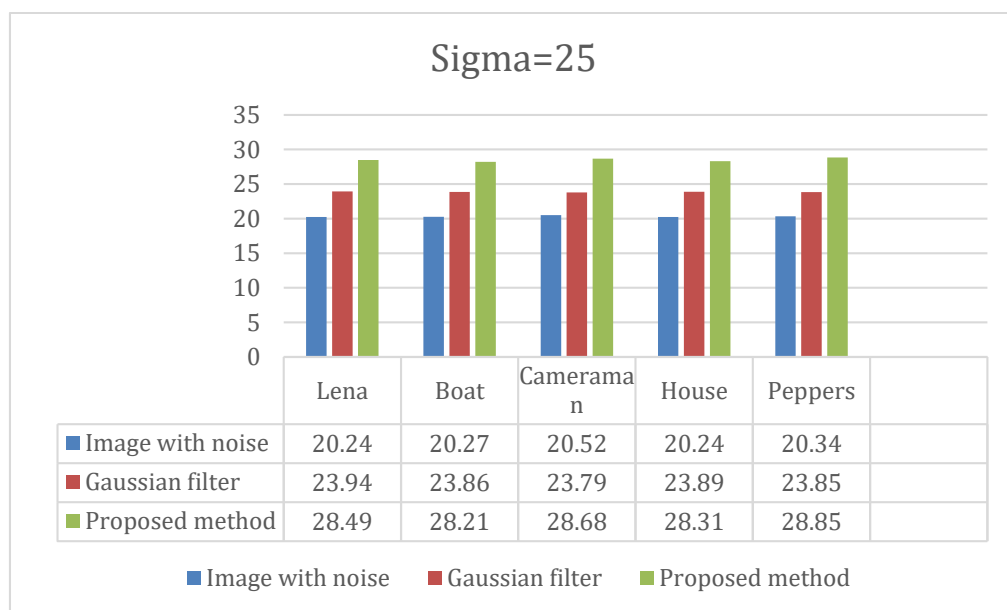


Figure 14. The PSNR of testing denoising result using Gaussian noise levels ( $\sigma = 25$ ) for grayscale images.

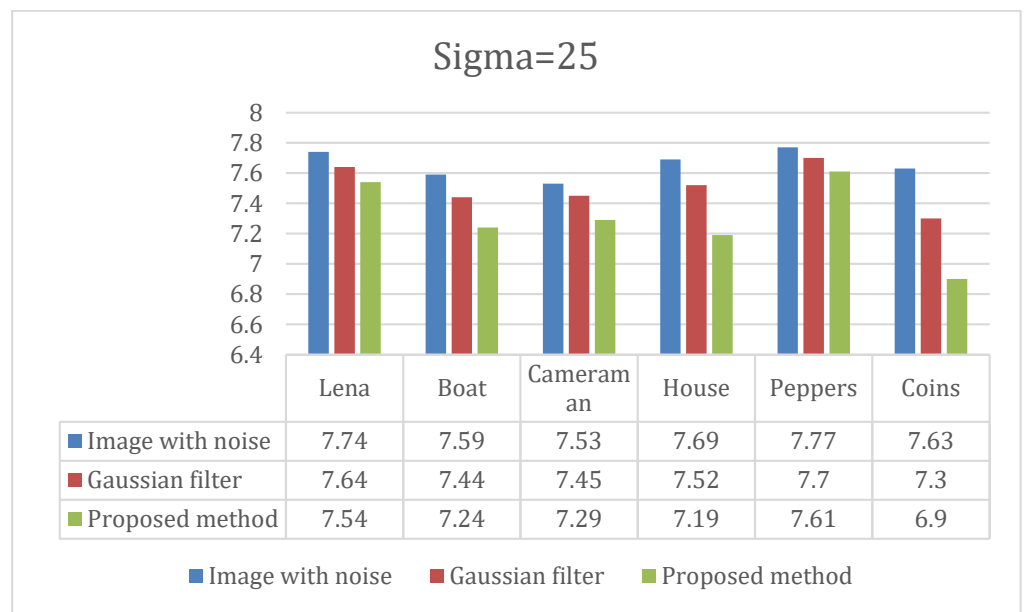


Figure 15. The entropy of testing denoising result using Gaussian noise levels ( $\sigma = 25$ ) for grayscale images.

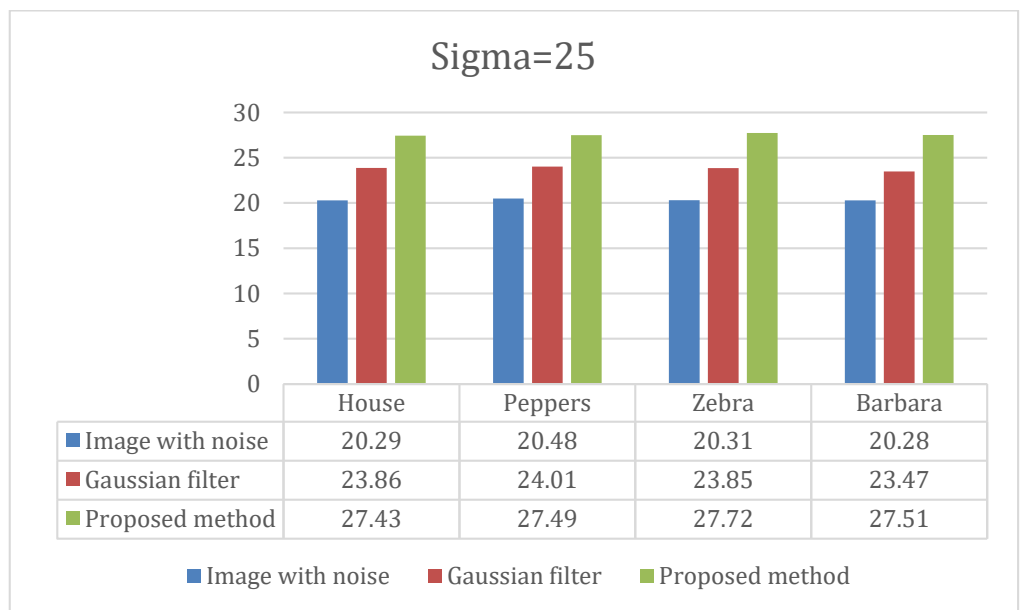


Figure 16. The PSNR of testing denoising result using Gaussian noise levels ( $\sigma = 25$ ) for color images.

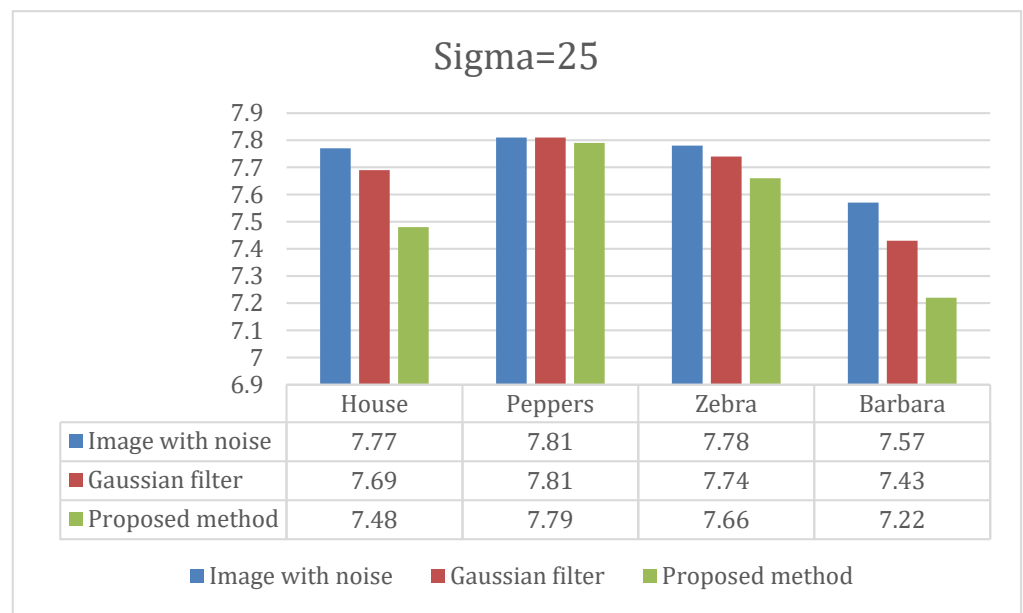


Figure 17. The entropy of testing denoising result using Gaussian noise levels ( $\sigma = 25$ ) for color images.



Figure 18. Cont.

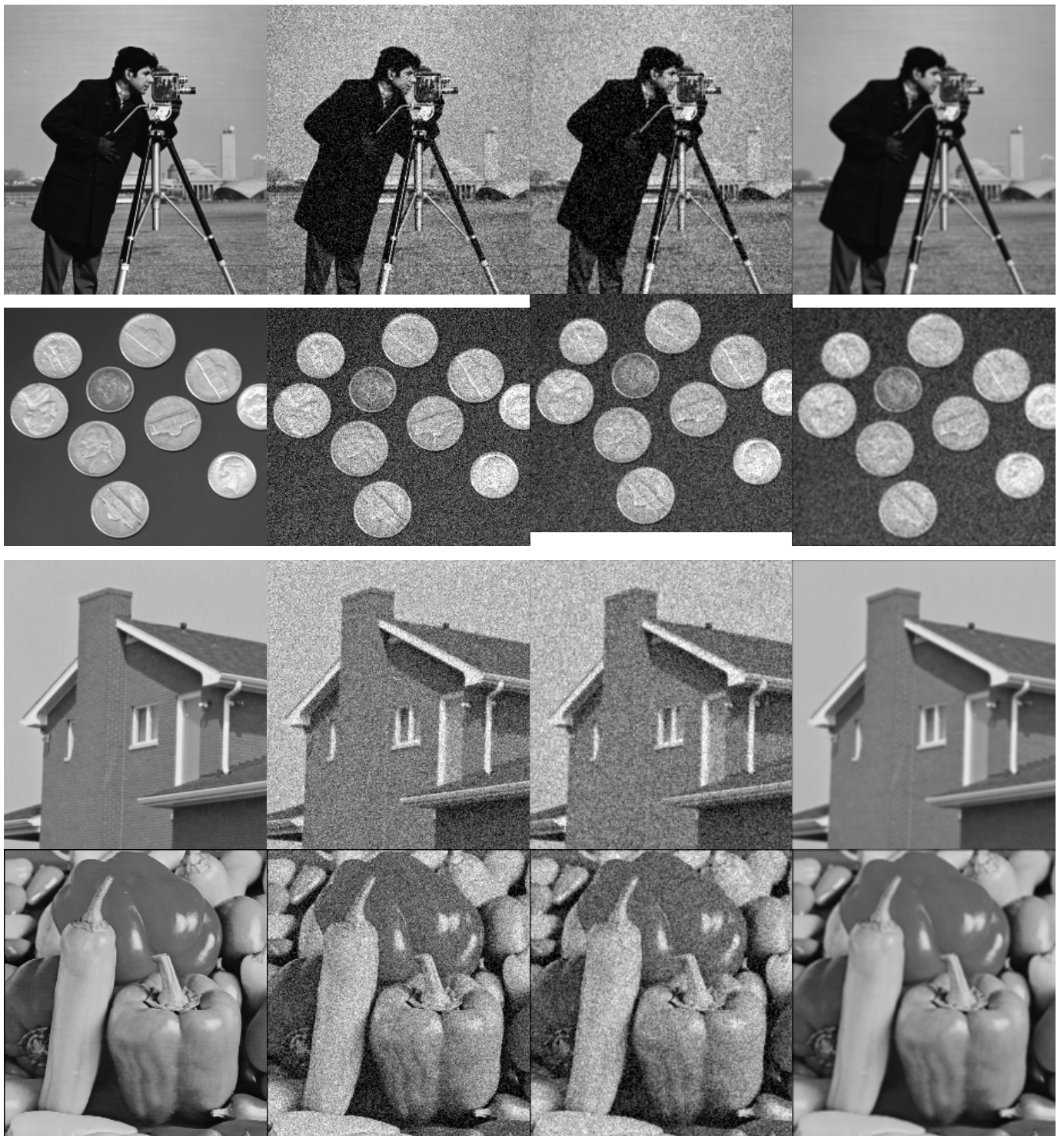


Figure 18. Cont.



Figure 18. The testing denoising result using Gaussian noise levels ( $\sigma = 30$ ).

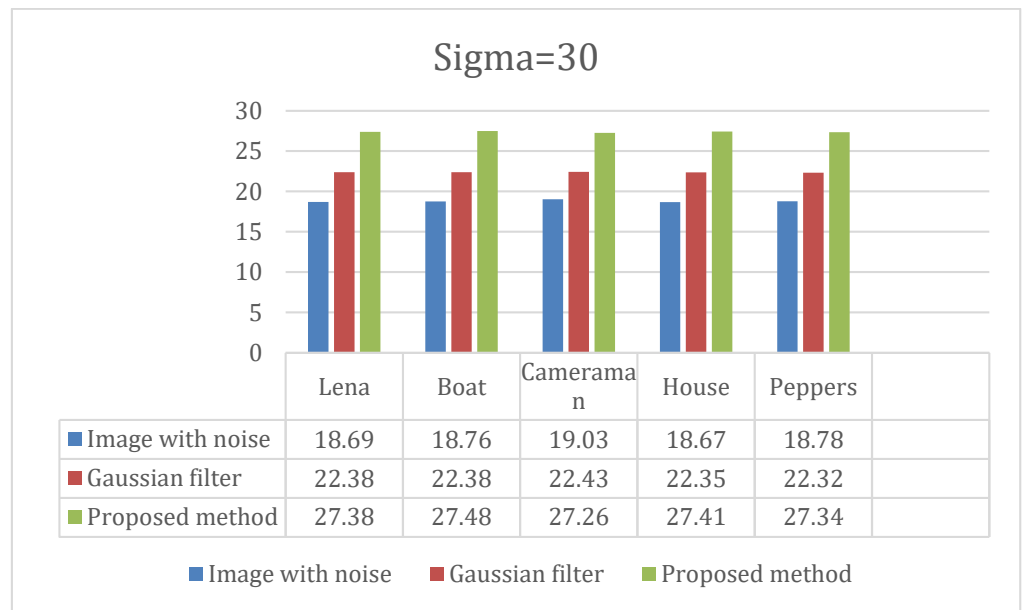


Figure 19. The PSNR of testing denoising result using Gaussian noise levels ( $\sigma = 30$ ) for grayscale images.

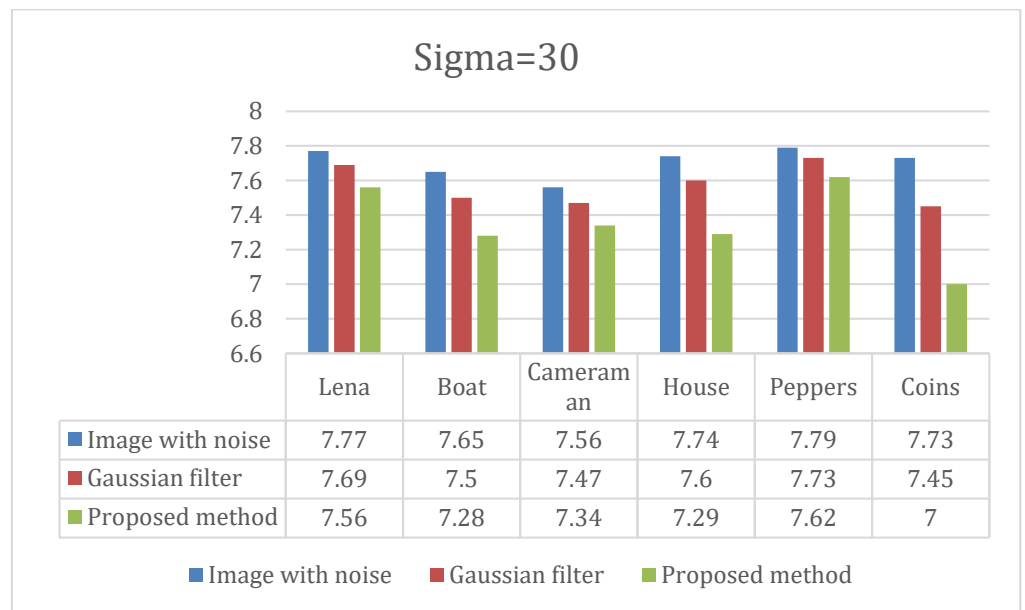
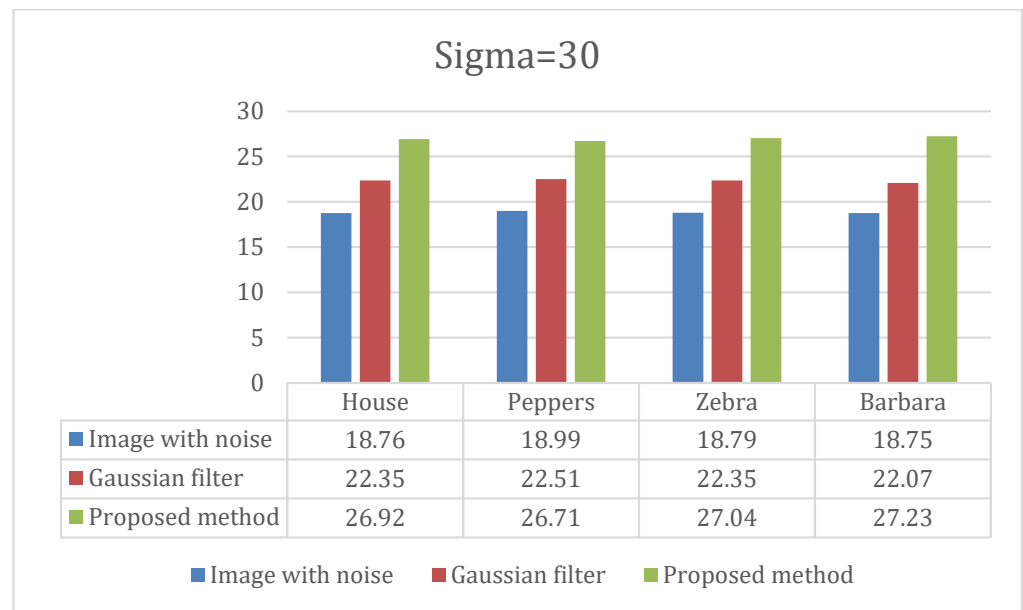


Figure 20. The entropy of testing denoising result using Gaussian noise levels ( $\sigma = 30$ ) for grayscale images.

It has been established through an experimental simulation that the suggested QC-LFE mask is compatible with the fractional parameter operators, which are empirically fixed at  $\mu = 0.1$  and  $q = 0.5$ . The performance metrics and the visual analysis are two factors that the current denoising evaluation methods use. The significance of artifacts, edge protection and texture reservation are the three main criteria for visual analysis for the human visual effect. The proposed denoising algorithm using the proposed QC-LFE mask has good denoising performance for both testing images by different degrees of Gaussian noise, as shown by all illustrations. Denoising of the image signal is gradually made more effective, and edge information is successfully extracted. It is obvious from observation that the denoising effect works best when  $\mu$  and  $q$  are between 0 and 1. Moreover, the denoised images obtained with various values of noise of  $\sigma$  for quantitative analysis exhibit the best denoised outcomes.





**Figure 21.** The PSNR of testing denoising result using Gaussian noise levels ( $\sigma = 30$ ) for color images.

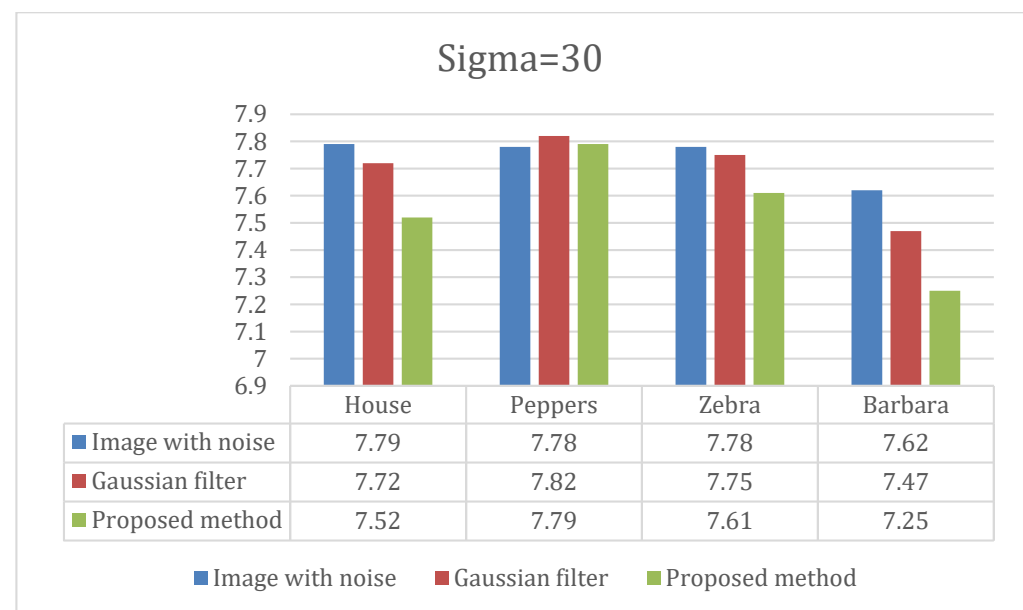


**Figure 22.** The entropy of testing denoising result using Gaussian noise levels ( $\sigma = 30$ ) for color images.

The maximum PSNR values (30.96) are obtained on the grayscale 'Lena' image, with Gaussian noise of  $\sigma = 15$ . The proposed method yielded acceptable denoising results. This revealed that the proposed fractional mask was helpful in minimizing the image noise.

The proposed image denoising algorithm for all testing images has a good denoising performance. The results of the experiments show that the denoising was compatible with the Gaussian standard smoothing filter. Additionally, the statistical measure of image pixel randomness that describes the texture of an image is known as entropy. The histogram of the image is used to calculate entropy across the entire image. According to the entropy results tables, the proposed mask has better denoising, and is adaptable to different levels of noise intensity. The obtained entropy results show that image detail information is maintained, while image noise has been decreased. The simulation results demonstrate that the proposed denoising algorithm model has a simple algorithm, is stable and can remove noise while preserving the details of an image's edge and texture.

From the discussion above, it is clear that the low-frequency features in the smooth area have been preserved, and the high-frequency edge has been enhanced in regions where the grayscale frequently changes.

## 5. The Comparative Analysis

To further demonstrate the efficacy of the suggested image denoising technique, the performance of the proposed QC-LFE method is tested on images affected by different Gaussian noise on a different grayscale, and is compared against existing state-of-the-art methods. The results are compared using the PSNR values. The following tables summarize previous studies that investigated the image denoising.

Based on the convex solution of the fractional heat equation, the study in [9] has used image denoising based on parameters of regularized fractionals. The method achieved a PSNR of 29.87 on the grayscale ‘Cameraman’ image.

For image denoising, other work by [10] has utilized fractional mask windows based on fractional Alexander polynomials. The achieved PSNR was 29.72 on the grayscale Pepper image.

The application of the approximate Cauchy-Euler equation solution proposed by [7] for image denoising achieved 30.96 PSNR for the grayscale ‘Lena’ image. Moreover, for image denoising, the Tsallis entropy with the Riesz fractional derivative was proposed by [11]. The achieved PSNR was 30.94 using the grayscale ‘Lena’ image. Likewise, the work in [14] applied a fractional integral operator with different types of entropies to improve the fractional masks. The achieved PSNR was 30.94 with the grayscale ‘Cameraman’ image. The proposed denoising method performed better than the previously mentioned five methods, as illustrated in Table 1 using grayscale ‘Lena’ image; Table 2 using grayscale ‘Boat’ image; Table 3 using grayscale ‘Cameraman’ image; Table 4 using grayscale ‘House’ image, and Table 5 using grayscale ‘Pepper’ image.

**Table 1.** Comparative study for the grayscale ‘Lena’ image.

Sigma( $\sigma$ )	Noisy Image	Method in [9]	Method in [10]	Method in [7]	Method in [11]	Method in [14]	Proposed Method
15	24.65	28.25	29.45	30.12	30.94	30.68	30.96
20	22.11	25.92	28.97	28.10	29.03	29.29	29.65
25	20.24	24.02	27.90	27.32	27.63	28.32	28.49
30	18.69	23.54	26.32	26.32	26.51	-	27.38

**Table 2.** Comparative study for the grayscale ‘Boat’ image.

Sigma( $\sigma$ )	Noisy Image	Method in [9]	Method in [10]	Method in [7]	Method in [11]	Method in [14]	Proposed Method
15	24.88	28.36	29.54	30.10	29.98	-	30.81
20	22.18	25.93	28.66	28.23	28.20	-	29.82
25	20.27	24.03	27.90	27.13	27.64	-	28.21
30	18.76	23.34	26.18	26.43	26.19	-	27.48

**Table 3.** Comparative study for the grayscale ‘Cameraman’ image.

Sigma( $\sigma$ )	Noisy Image	Method in [9]	Method in [10]	Method in [7]	Method in [11]	Method in [14]	Proposed Method
15	24.63	29.87	29.45	30.12	29.63	30.94	30.91
20	22.48	26.37	28.15	28.24	28.62	29.55	29.89
25	20.52	24.92	26.47	27.35	27.09	28.38	28.68
30	19.03	23.01	25.81	26.38	26.24	-	27.26

**Table 4.** Comparative study for the grayscale ‘House’ image.

Sigma( $\sigma$ )	Noisy Image	Method in [9]	Method in [10]	Method in [7]	Method in [11]	Method in [14]	Proposed Method
15	24.68	28.34	29.18	29.32	31.76	-	30.85
20	22.15	25.92	26.64	28.62	29.58	-	29.18
25	20.24	24.02	26.61	27.81	27.83	-	28.31
30	18.67	23.51	25.42	26.51	26.68	-	27.41

**Table 5.** Comparative study for the grayscale ‘Pepper’ image.

Sigma( $\sigma$ )	Noisy Image	Method in [9]	Method in [10]	Method in [7]	Method in [11]	Method in [14]	Proposed Method
15	24.62	28.51	29.72	29.61	29.16	29.97	30.76
20	22.24	26.08	26.97	28.37	27.83	28.85	29.96
25	20.34	24.17	26.83	27.29	27.47	27.72	28.85
30	18.78	23.65	25.86	26.43	26.57	-	27.34

The proposed denoising method performed the best, particularly under different Gaussian noise levels, though a high level of noise will disturb pixel probability. The proposed denoising method, however, dealt with noise effectively as it makes use of pixel probability data with a fractional mask convolution operation. The proposed study was successful in removing image noise with a PSNR of 30.96, which can be used as a pre-processing stage for many image-processing applications.

All tables show that the PSNR value of the proposed image denoising method is higher than that of the other denoising models mentioned. Using quantum calculus with local fractional entropy for image denoising described the relationship of gray levels between neighboring pixels. The proposed mathematical method, which was thought to be important for removing image noise, was able to enhance the image quality. The main drawback of this study is that the proposed denoising method does not perform well on edges of images; instead, it does well on flat portions of images.

## 6. Conclusions

In this study, the fractional denoising algorithm was proposed based on the quantum calculus of local fractional entropy (QC-LFE), which was the key to this denoising method. The mask coefficients were determined by the intensity of the local fractional entropy, which protected the edge and texture details of denoised images. The proposed denoising algorithm used a processing fractional mask with  $n \times n$  elements. The suggested image denoising algorithm processes corrupted each pixel one at a time using mask convolution. The denoising ability of QC-LFE was reliable in comparison to other fractional operators, according to the evaluation indicators. The achieved PSNR measures are all higher under different values of noise. The experimental results confirm that the proposed QC-LFE had improved the input images and preserved texture details efficiently. Moreover, some other kinds of quantum calculus-fractional entropy-based denoising algorithms are worth being studied in future work.

**Author Contributions:** Conceptualization, A.R.A.-S.; methodology, R.W.I.; software, A.R.A.-S.; validation, R.W.I. and A.R.A.-S.; formal analysis, R.W.I.; writing—original draft preparation, A.R.A.-S.; and writing—review and editing, R.W.I. All authors have read and agreed to the published version of the manuscript.

**Funding:** This research received no external funding.

**Data Availability Statement:** Not applicable.

**Acknowledgments:** The authors would like to acknowledge the support of Prince Sultan University for paying the Article Processing Charge (APC) of this publication and their support.

**Conflicts of Interest:** The authors declare no conflict of interest.

## References

1. Noor, A.; Zhao, Y.; Khan, R.; Wu, L.; Abdalla, F.Y. Median filters combined with denoising convolutional neural network for Gaussian and impulse noises. *Multimed. Tools Appl.* **2020**, *79*, 18553–18568. [[CrossRef](#)]
2. Fan, L.; Zhang, F.; Fan, H.; Zhang, C. Brief review of image denoising techniques. *Vis. Comput. Ind. Biomed. Art* **2019**, *2*, 7. [[CrossRef](#)] [[PubMed](#)]
3. Ibrahim, R.W.; Moghaddasi, Z.; Jalab, H.A.; Noor, R.M. Fractional differential texture descriptors based on the Machado entropy for image splicing detection. *Entropy* **2015**, *17*, 4775–4785. [[CrossRef](#)]
4. Jalab, H.A.; Subramaniam, T.; Ibrahim, R.W.; Kahtan, H.; Noor, N.F.M. New texture descriptor based on modified fractional entropy for digital image splicing forgery detection. *Entropy* **2019**, *21*, 371. [[CrossRef](#)] [[PubMed](#)]
5. Subramaniam, T.; Jalab, H.A.; Ibrahim, R.W.; Mohd Noor, N.F. Improved image splicing forgery detection by combination of conformable focus measures and focus measure operators applied on obtained redundant discrete wavelet transform coefficients. *Symmetry* **2019**, *11*, 1392. [[CrossRef](#)]
6. Wang, Q.; Ma, J.; Yu, S.; Tan, L. Noise detection and image denoising based on fractional calculus. *Chaos Solitons Fractals* **2020**, *131*, 109463. [[CrossRef](#)]
7. Ibrahim, R.; Jalab, H. Image denoising based on approximate solution of fractional Cauchy-Euler equation by using complex-step method. *Iran. J. Sci. Technol.* **2015**, *39*, 243.
8. Ibrahim, R.W.; Elobaid, R.M.; Obaiys, S.J. Geometric inequalities via a symmetric differential operator defined by quantum calculus in the open unit disk. *J. Funct. Spaces* **2020**, *2020*, 6932739. [[CrossRef](#)]
9. Jalab, H.A. Regularized fractional power parameters for image denoising based on convex solution of fractional heat equation. In *Abstract and Applied Analysis*; Hindawi: London, UK, 2014.
10. Jalab, H.A.; Ibrahim, R.W. Fractional Alexander polynomials for image denoising. *Signal Process.* **2015**, *107*, 340–354. [[CrossRef](#)]
11. Jalab, H.A.; Ibrahim, R.W.; Ahmed, A. Image denoising algorithm based on the convolution of fractional Tsallis entropy with the Riesz fractional derivative. *Neural Comput. Appl.* **2017**, *28*, 217–223. [[CrossRef](#)]
12. Yu, J.; Tan, L.; Zhou, S.; Wang, L.; Wang, C. Image denoising based on adaptive fractional order anisotropic diffusion. *KSII Trans. Internet Inf. Syst. (TIIS)* **2017**, *11*, 436–450.
13. Ibrahim, R.W. A new image denoising model utilizing the conformable fractional calculus for multiplicative noise. *SN Appl. Sci.* **2020**, *2*, 32. [[CrossRef](#)]
14. Lin, X.; Wang, Y.; Wu, G.; Hao, J. Image denoising of adaptive fractional operator based on Atangana–Baleanu derivatives. *J. Math.* **2021**, *2021*, 5581944. [[CrossRef](#)]
15. El-Shafai, W.; Mahmoud, A.; Ali, A.; El-Rabaie, E.; Taha, T.; Zahran, O.; El-Fishawy, A.; Soliman, N.; Alhussan, A.; Abd El-Samie, F. Deep CNN Model for Multimodal Medical Image Denoising. *Comput. Mater. Contin* **2022**, *73*, 3795–3814. [[CrossRef](#)]
16. Yao, C.; Tang, Y.; Sun, J.; Gao, Y.; Zhu, C. Multiscale residual fusion network for image denoising. *IET Image Process.* **2022**, *16*, 878–887. [[CrossRef](#)]
17. Yang, X.-J.; Baleanu, D.; Srivastava, H. Local fractional similarity solution for the diffusion equation defined on Cantor sets. *Appl. Math. Lett.* **2015**, *47*, 54–60. [[CrossRef](#)]
18. Yang, X.-J.; Srivastava, H.; He, J.-H.; Baleanu, D. Cantor-type cylindrical-coordinate method for differential equations with local fractional derivatives. *Phys. Lett. A* **2013**, *377*, 1696–1700. [[CrossRef](#)]
19. Yang, X.-J. *Local Fractional Functional Analysis & Its Applications*; Citeseer: Hong Kong, China, 2011.
20. Cattani, C. Cantor Waves for Signorini Hyperelastic Materials with Cylindrical Symmetry. *Axioms* **2020**, *9*, 22. [[CrossRef](#)]
21. Yang, X.-J. Local fractional partial differential equations with fractal boundary problems. *Adv. Comput. Math. Its Appl.* **2012**, *1*, 60–63.
22. Ernst, T. *A Comprehensive Treatment of Q-Calculus*; Springer Science & Business Media: Birkhäuser Basel, 2012.
23. Ernst, T. *The History of Q-Calculus and a New Method*; Citeseer: Hong Kong, China, 2000.
24. Berg, C. On a generalized Gamma convolution related to the q-calculus. In *Theory and Applications of Special Functions*; Springer: Berlin/Heidelberg, Germany, 2005; pp. 61–76.
25. Berg, C. THE q-CALCULUS. *Theory Appl. Spec. Funct. A Vol. Dedic. Mizan Rahman* **2006**, *13*, 61.
26. Exton, H.; Srivastava, H. A certain class of q-Bessel polynomials. *Math. Comput. Model.* **1994**, *19*, 55–60. [[CrossRef](#)]
27. Kac, V.G.; Cheung, P. *Quantum Calculus*; Springer: Berlin/Heidelberg, Germany, 2002; Volume 113.
28. Rashid, S.; Hammouch, Z.; Ashraf, R.; Baleanu, D.; Nisar, K.S. New quantum estimates in the setting of fractional calculus theory. *Adv. Differ. Equ.* **2020**, *2020*, 383. [[CrossRef](#)]
29. Ma, Y.; Ma, H.; Chu, P. Demonstration of quantum image edge extraction enhancement through improved Sobel operator. *IEEE Access* **2020**, *8*, 210277–210285. [[CrossRef](#)]
30. Fink, T.; Kähler, U. A space-based method for the generation of a schwartz function with infinitely many vanishing moments of higher order with applications in image processing. *Complex Anal. Oper. Theory* **2019**, *13*, 985–1010. [[CrossRef](#)]
31. Al-Saidi, N.M.; Yahya, H.; Obaiys, S.J. Discrete Dynamic Model of a Disease-Causing Organism Caused by 2D-Quantum Tsallis Entropy. *Symmetry* **2022**, *14*, 1677. [[CrossRef](#)]
32. Samei, M.E.; Zanganeh, H.; Aydogan, S.M. To investigate a class of the singular fractional integro-differential quantum equations with multi-step methods. *J. Math. Ext.* **2021**, *15*, 1–54. [[CrossRef](#)]

33. Yue, X.-G.; Samei, M.E.; Fathipour, A.; Kaabar, M.K.; Kashuri, A. Using Krasnoselskii's theorem to investigate the Cauchy and neutral fractional  $q$ -integro-differential equation via numerical technique. *Nonlinear Eng.* **2022**, *11*, 186–206. [[CrossRef](#)]
34. Ali, K.; TAŞBOZAN, O. A New Concept for Fractional Quantum Calculus:(B;  $q$ )-Calculus and Its Properties. *Ikonion J. Math.* **2020**, *2*, 44–48.

**Disclaimer/Publisher's Note:** The statements, opinions and data contained in all publications are solely those of the individual author(s) and contributor(s) and not of MDPI and/or the editor(s). MDPI and/or the editor(s) disclaim responsibility for any injury to people or property resulting from any ideas, methods, instructions or products referred to in the content.